Coordination between the circadian clock and androgen signaling is required to sustain rhythmic expression of *Elovl3* in mouse liver

Received for publication, September 20, 2018, and in revised form, February 19, 2019 Published, Papers in Press, March 12, 2019, DOI 10.1074/jbc.RA118.005950

Huatao Chen (陈 华涛)[‡§1,2], **Lei Gao** (高 磊)[‡§1], **Dan Yang** (杨 丹)[‡§3], **Yaoyao Xiao** (肖 要要)[‡§], **Manhui Zhang** (张 漫慧)[‡§], **Cuimei Li** (李 翠梅)[‡§], **Aihua Wang** (王 爱华)[§¶], **and Yaping Jin** (靳 亚平)[‡§4]

From the Departments of [‡]Clinical Veterinary Medicine and [¶]Preventive Veterinary Medicine, College of Veterinary Medicine, and the [§]Key Laboratory of Animal Biotechnology of the Ministry of Agriculture, Northwest A&F University, Yangling, 712100 Shaanxi, China

Edited by Qi-Qun Tang

ELOVL3 is a very long-chain fatty acid elongase, and its mRNA levels display diurnal rhythmic changes exclusively in adult male mouse livers. This cyclical expression of hepatic *Elovl3* is potentially controlled by the circadian clock, related hormones, and transcriptional factors. It remains unknown, however, whether the circadian clock, in conjunction with androgen signaling, functions in maintaining the rhythmic expression of *Elovl3* in a sexually dimorphic manner. Under either zeitgeber or circadian time, WT mouse livers exhibited a robust circadian rhythmicity in the expression of circadian clock genes and *Elovl3*. In contrast, male *Bmal1*$^{-/-}$ mice displayed severely weakened expression of hepatic circadian clock genes, resulting in relatively high, but nonrhythmic, *Elovl3* expression levels. ChIP assays revealed that NR1D1 binds to the *Elovl3* promoter upon circadian change in WT mouse livers *in vivo*, and a diminished binding was observed in male *Bmal1*$^{-/-}$ mouse livers. Additionally, female mouse livers exhibited constant low levels of *Elovl3* expression. Castration markedly reduced *Elovl3* expression levels in male mouse livers but did not disrupt circadian variation of *Elovl3*. Injection of female mice with 5α-dihydrotestosterone induced *Elovl3* rhythmicity in the liver. In AML12 cells, 5α-dihydrotestosterone also elevated *Elovl3* expression in a time-dependent manner. In contrast, flutamide efficiently attenuated this induction effect. In conclusion, a lack of either the circadian clock or androgen signaling impairs hepatic *Elovl3* expression, highlighting the observation that coordination between the circadian clock and androgen signaling is required to sustain the rhythmic expression of *Elovl3* in mouse liver.

Elovl3 (elongation of very long-chain fatty acids 3), also known as *Cig30*, was initially identified as a thermogenesis-related gene after its expression in brown adipose tissue was found to be highly elevated in response to cold stimulation (1). Accumulating reports indicate that significant *Elovl3* expression also occurs in white adipose tissue, liver, and triglyceride-rich glands, such as the sebaceous and meibomian glands (2–5). As a member of the *Elovl* gene family, *Elovl3* encodes an enzyme that functions in the synthesis of C20–C24 saturated and mono-unsaturated very long-chain fatty acids (VLCFAs).[5] It was previously demonstrated that *Elovl3*$^{-/-}$ mice exhibit a clear skin phenotype with an impaired barrier function resulting from changes in the synthesis of C20–C24 saturated and mono-unsaturated VLCFAs, triglyceride synthesis, and sebum formation (5). Male *Elovl3*$^{-/-}$ mice also display a diminished capacity to accumulate fat within brown adipose tissue (6). Additionally, male and female *Elovl3*$^{-/-}$ mice possess reduced hepatic lipogenic gene expression and triglyceride content and are also resistant to diet-induced obesity (7). These findings indicate that ELOVL3 acts as an important regulator of triglyceride and lipid droplet formation in skin, adipose tissue, and liver. To further determine the physiological significance of *Elovl3*, an increasing number of studies aim to clarify its upstream regulatory mechanisms (2–4, 8, 9). Interestingly, it was observed that VLCFAs enhance adipogenesis through the co-regulation of ELOVL3 and PPARγ in 3T3-L1 adipocytes (9). It was also found that vitamin D/vitamin D nuclear hormone receptor modulates the fatty acid composition in mouse subcutaneous white adipose tissue through the direct inhibition of *Elovl3* expression (2). Additionally, several elegant reports provided evidence that *Elovl3* expression exhibits a robust circa-

This work was supported by National Natural Science Foundation of China Grants 31771301 and 31602125 (to H. C.) and 31772817 (to Y. J.), China Postdoctoral Science Foundation Grants 2017M61065 and 2018T111112 (to H. C.), Shaanxi Postdoctoral Science Foundation Grant 2017BSHEDZZ105 (to H. C.), Fundamental Research Funds for the Central Universities Grant 2452017292 (to H. C.), Scientific Research Foundation for Talents of Shaanxi Grant A279021712 (to H. C.), and Scientific Research Foundation for Talents of Northwest A&F University Grant Z11021601 (to H. C.). The authors declare that they have no conflicts of interest with the contents of this article.

This article contains Fig. S1.

[1] Both authors contributed equally to this work.

[2] To whom correspondence may be addressed: Dept. of Clinical Veterinary Medicine, College of Veterinary Medicine, Northwest A&F University, Yangling, 712100 Shaanxi, China. Tel.: 86-18049052038; E-mail: htchen@nwafu.edu.cn.

[3] Present address: Laboratory of Regulation in Metabolism and Behavior, Graduate School of Agriculture, Kyushu University, Fukuoka, Japan.

[4] To whom correspondence may be addressed: Dept. of Clinical Veterinary Medicine, College of Veterinary Medicine, Northwest A&F University, Yangling, 712100 Shaanxi, China. Tel.: 86-13474069788; E-mail: yapingjin@163.com.

[5] The abbreviations used are: VLCFA, very long-chain fatty acid; CCG, clock-controlled gene; RORE, REV-ERBs/RORs response element (RORE); ZT, zeitgeber time; CT, circadian time; DHT, 5α-dihydrotestosterone; DD, constant darkness; LD, light-dark; qPCR, quantitative real-time PCR; ANOVA, analysis of variance.

dian rhythmicity in mouse livers, where *Clock* mutant mice possess a constant but relatively high level of hepatic *Elovl3* expression (3, 4, 10).

The circadian clock system is ubiquitous in nearly all mammalian organs, tissues, and cells (11), where it orchestrates numerous physiological functions and behaviors within the body (12). The central pacemaker of the circadian clock resides in the suprachiasmatic nucleus of the hypothalamus (13), which regulates the subsidiary circadian oscillators in peripheral tissues and cells via humoral and neuronal cues in a hierarchical manner (14, 15). Molecularly, the suprachiasmatic nucleus and peripheral circadian oscillators share an interlocked transcriptional-translational feedback loop involving a set of canonical circadian clock genes, including *Bmal1*, *Clock*, *Per1/Per2/Per3*, *Cry1/Cry2*, *Nr1d1*, and *Dbp* (16). In addition to maintaining oscillations of circadian clock, the proteins encoded by circadian clock genes (BMAL1, CLOCK, NR1D1, and DBP) also maintain the rhythmic expression of clock-controlled genes (CCGs) through binding to promoter E-box, REV-ERBs/RORs response element (RORE), and D-box elements. Using cDNA microarray or Northern blot analysis, prior reports have shown that a diurnal cyclical expression of *Elovl3* exists in male mouse liver (3, 4, 10). Clock mutation results in nonrhythmic expression and a marginal increase in the levels of *Elovl3* expression in male mouse livers (4, 10). These findings suggest that *Elovl3* is a potential CCG. Despite one previous study providing plausible evidence that the circadian clock regulates *Elovl3* expression through NR1D1 inhibition (4), additional studies are required to understand and verify this proposed mechanism.

Sexual dimorphism is a common feature of male and female mouse liver. Existing evidence indicates that distinct sex hormone (androgens and estrogens) signaling, and the resulting growth hormone signaling, in the male and female liver are major diving factors underlying this hepatic sexual dimorphism (17, 18). In a recent study, a total of 6612 differentially expressed genes exhibiting at least a 1.5-fold change were identified between male and female mouse livers (19). Intriguingly, two aforementioned studies demonstrated that *Elovl3* belongs to the family of hepatic sexually dimorphic genes, with high and rhythmic expression being observed in male mouse livers and undetectable or low expression in female mouse livers (3, 4). This suggests that androgen signaling might play an essential role in determining the hepatic sexual dimorphism of *Elovl3* expression; however, evidence is lacking regarding whether androgen complementation elicits hepatic *Elovl3* expression in female mouse livers *in vivo* or if androgen treatment of hepatocytes increases *Elovl3* expression *in vitro*. Further studies are urgently required to address these issues.

Here, we demonstrate that under zeitgeber time (ZT) or circadian time (CT) conditions, male *Bmal1*$^{-/-}$ mice exhibited nonrhythmic expression of *Elovl3* in liver while maintaining *Elovl3* expression at relatively high levels. This was in contrast to observations of male WT mouse livers, where robust circadian rhythmicity in *Elovl3* expression was observed to exhibit anti-phase circadian variations with respect to *Nr1d1*. ChIP assays indicated that NR1D1 was recruited to a putative RORE site at the *Elovl3* promoter in a circadian manner in male WT mice livers *in vivo*, and this was attenuated in *Bmal1*$^{-/-}$ mice. In addition, we confirmed that *Elovl3* is a hepatic sexually dimorphic gene exhibiting high and rhythmic expression in male mice and low and constant expression in female mice. Although it did not profoundly alter the expression of circadian clock genes, castration greatly decreased *Elovl3* expression in mouse liver. 5α-Dihydrotestosterone (DHT) treatment of female mice not only vastly elevated *Elovl3* expression at CT0 and restored its circadian rhythmicity in female mouse liver *in vivo*, but *in vitro*, it also significantly increased the expression of *Elovl3* in AML12 cells in a time-dependent manner. Flutamide treatment also efficiently reduced *Elovl3* expression induced by DHT in AML12 cells. Our current study therefore provides novel findings that extend our current understanding of how the circadian clock and androgen signaling synergistically regulate rhythmic *Elovl3* expression in mouse liver, highlighting the significance of circadian clock and androgen signaling in coordinating hepatic lipid metabolism.

Results

Loss of BMAL1 results in hepatic triglyceride accumulation and elevated and arrhythmic Elovl3 expression

To investigate the physiological role of the circadian clock in regulating murine hepatic *Elovl3* mRNA expression and its associated hepatic lipid metabolism, we used *Bmal1*$^{-/-}$ mice and their WT siblings (control). PCR genotyping of tail biopsies, immunohistochemistry, and Western blot analysis were initially used to confirm complete deficiency of BMAL1 protein in *Bmal1*$^{-/-}$ mice compared with WT (Fig. S1, *A–C*). As expected, *Bmal1*$^{-/-}$ mice completely lost circadian locomotor activity in constant darkness (DD), whereas day–night rhythms were observed under light– dark (LD) cycles due to the masking effect of the environmental lighting cycle (Fig. S1*D*). Additionally, Oil Red O staining for neutral lipids was increased in livers of male *Bmal1*$^{-/-}$ mice (Fig. 1*A*), and the hepatic triglyceride content was nearly double that of WT mice (Fig. 1*B*).

We then examined the temporal expression profiles of several circadian clock genes (*Bmal1*, *Nr1d1*, and *Dbp*) and *Elovl3* in the livers of male WT and *Bmal1*$^{-/-}$ mice. As shown in Fig. 1 (*C* and *D*), *Bmal1*$^{-/-}$ mice exhibited undetectable hepatic *Bmal1* expression compared with the robust circadian rhythmicity of *Bmal1* observed in WT mice under both ZT and CT conditions (Cosinor analysis, $p < 0.001$). Indeed, in WT mice, both the *Nr1d1* and *Dbp* transcripts exhibited a cyclical expression pattern (Cosinor analysis, $p < 0.001$) that was opposite that of the *Bmal1* expression profile (Fig. 1, *C* and *D*). In contrast, in WT mice hepatic *Elovl3* mRNA exhibited a similar expression pattern to that of *Bmal1*, with a trough of expression at ZT12 (Fig. 1, *C* and *D*). In *Bmal1*$^{-/-}$ mice, the loss of BMAL1 not only greatly inhibited hepatic *Nr1d1* mRNA expression but also led to its nonrhythmic expression (Fig. 1, *C* and *D*). Interestingly, the expression of *Dbp* was significantly attenuated and phase-shifted in *Bmal1*$^{-/-}$ mouse liver under ZT conditions (Fig. 1*C*); however, *Dbp* expression maintained its circadian rhythmicity (Cosinor analysis, $p < 0.01$). The expression of *Dbp* was remarkably suppressed and completely lost its circadian rhythmicity in *Bmal1*$^{-/-}$ mice under CT conditions (Fig. 1*D*). It should be noted that the diurnal rhythmic expression profile of

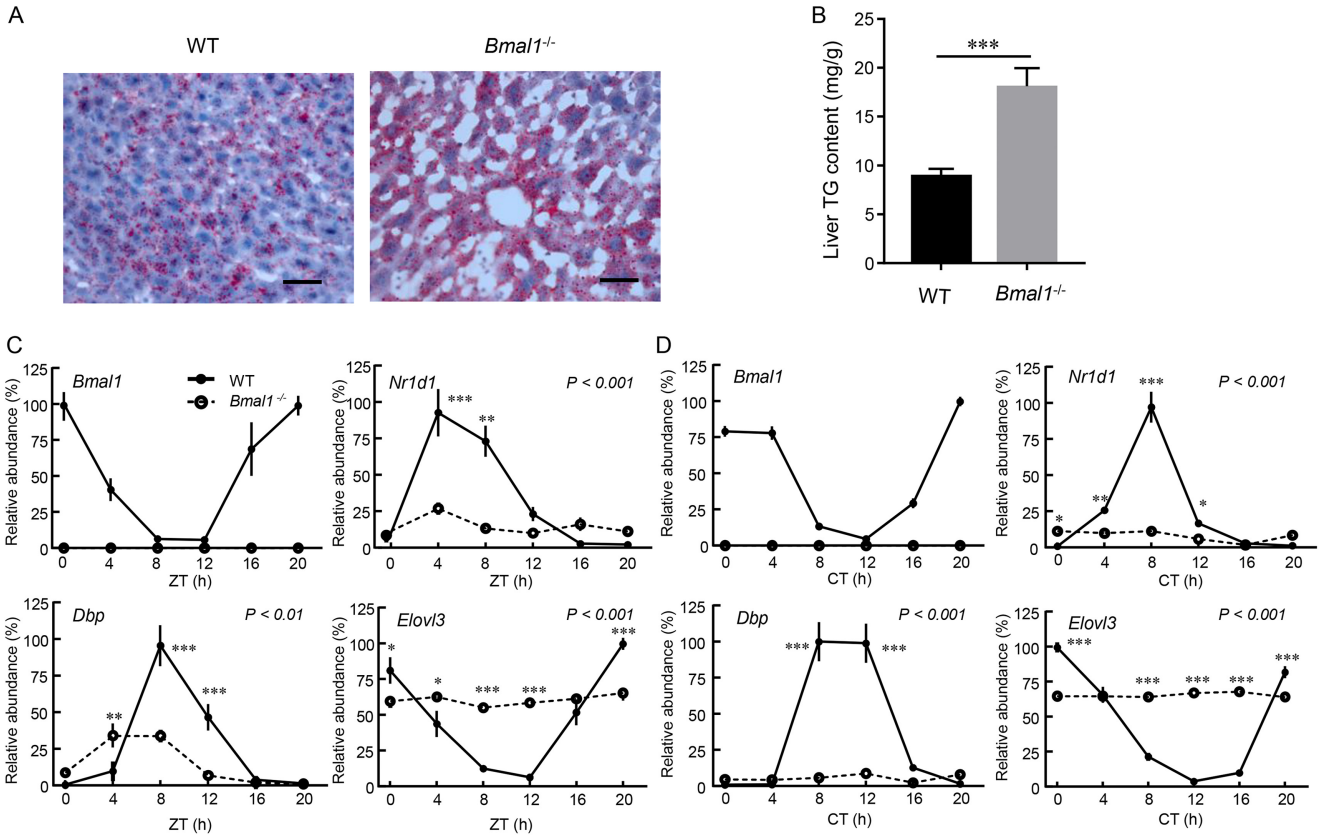

Figure 1. Loss of BMAL1 results in elevated hepatic triglyceride accumulation and arrhythmic *Elovl3* expression. *A*, representative Oil Red O staining of male WT and *Bmal1*$^{-/-}$ mouse liver tissue samples. Liver tissue samples were excised at ZT10. *Scale bar*, 20 μm. *B*, triglyceride contents in the livers of male WT and *Bmal1*$^{-/-}$ mice. Liver tissue samples were excised at ZT10. Data represent the means ± S.E. (*error bars*) ($n = 8$ for each genotype). *Asterisks* indicate significant differences. ***, $p < 0.001$. *C* and *D*, expression profiles of mRNAs for circadian clock genes and *Elovl3* in the livers of male WT and *Bmal1*$^{-/-}$ mice under both ZT and CT conditions. Total RNA was extracted from the livers of male WT and *Bmal1*$^{-/-}$ mice collected at the indicated time points, and the mRNA levels were quantified by qPCR. The mRNA levels were corrected relative to the levels of two reference genes (*Tbp* and *36b4*). The maximum expression level for each gene in the WT mice is expressed as 100%. Each value represents the mean ± S.E. of three independent determinations. A two-way ANOVA with Bonferroni's post-test was performed to investigate the main effects of genotype on the expression of the genes examined. Differences were considered significant at $p < 0.05$. *Asterisks* indicate significant differences between WT and *Bmal1*$^{-/-}$ mice at the indicated time points. *, $p < 0.05$; **, $p < 0.01$; ***, $p < 0.001$.

Elovl3 was completely abolished in the livers of *Bmal1*$^{-/-}$ mice, with significant, but constant, levels of expression being noted, where elevated levels were observed at ZT4, ZT8, and ZT12 compared with those of WT mice (Fig. 1*C*). Similarly, the expression levels of *Elovl3* were constant, with elevated levels observed at CT8, CT12, and CT16 compared with those of WT mice (Fig. 1*D*).

Diurnal recruitment of NR1D1 to the Elovl3 promoter in mouse liver in vivo

NR1D1, also known as REV-ERBα, is a nuclear hormone–related protein that functions as a transcriptional repressor of its target genes (20, 21). A computational algorithm (http://jaspar.genereg.net/)[6] (44) identified a putative RORE site within the *Elovl3* promoter between −831 and −841 (Fig. 2*A*). To determine whether NR1D1 binds to the *Elovl3* putative RORE site in mouse liver with a circadian change, we performed ChIP assays using a NR1D1 antibody in the livers of male WT and *Bmal1*$^{-/-}$ mice using samples collected at two representative time points (CT8 and CT20). *Bmal1*-RORE was used as a validated positive control (22), and a DNA region located in the first intron of *Elovl3* was used as a negative control (Fig. 2*A*). ChIP results revealed NR1D1 binding to the genomic *Elovl3*-RORE of WT mouse livers with a circadian change (Fig. 2*B*) that was similar to that of *Bmal1*-RORE, with strong binding at CT8 and weak binding at CT20. Additionally, NR1D1 recruitment was diminished at both *Elovl3*-RORE and *Bmal1*-RORE in *Bmal1*$^{-/-}$ mice, consistent with the dramatic reduction of *Nr1d1* mRNA levels observed in *Bmal1*$^{-/-}$ mice.

Sexually dimorphic pattern of Elovl3 expression in mouse liver

To determine whether there is sexual dimorphism in hepatic *Elovl3* expression, we determined the expression profile of *Elovl3*, as well as three other canonical clock genes (*Bmal1*, *Per2*, and *Dbp*), in male and female WT mouse livers at two representative time points (CT0 and CT12) using a quantitative real-time PCR (qPCR) assay. The results are shown in Fig. 3. All clock genes examined exhibited robust circadian changes in their mRNA expression in both male and female mouse livers (Fig. 3). Additionally, *Per2* and *Dbp* exhibited the expected antiphase circadian variations with respect to *Bmal1* (Fig. 3). It should be noted that hepatic *Elovl3* expression exhibited a clear sexual dimorphism, with a constant low level of expression

[6] Please note that the JBC is not responsible for the long-term archiving and maintenance of this site or any other third party hosted site.

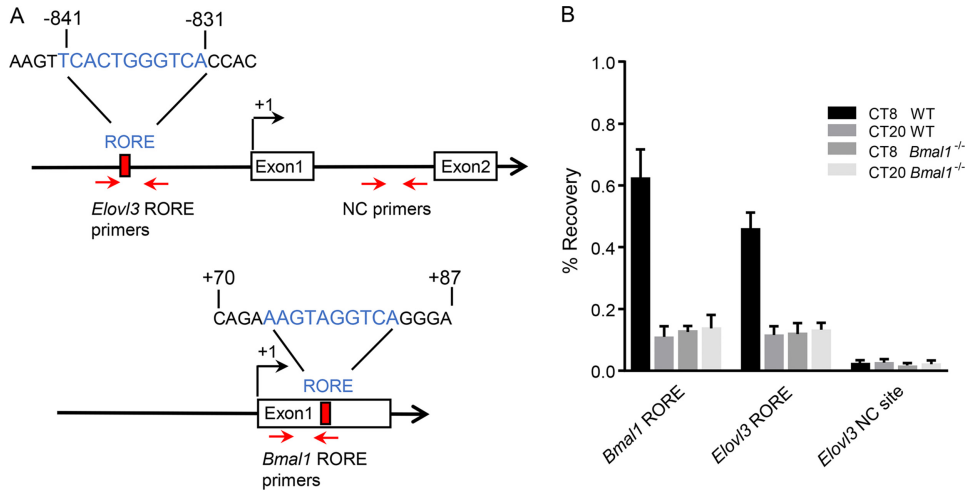

Figure 2. ChIP-PCR for NR1D1 in male WT and *Bmal1*$^{-/-}$ mice livers. *A*, ChIP regions are schematically shown on the *Elovl3* promoter, *Elovl3* intron 1, and the *Bmal1* promoter. The *Elovl3* intron 1 is a negative control (*NC*) region, and the *Bmal1* promoter is a validated positive control region. *B*, NR1D1 ChIP on liver extracts harvested at CT8 and CT20 from male WT and *Bmal1*$^{-/-}$ mice ($n = 4$ for each genotype and time point). *Error bars*, S.E.

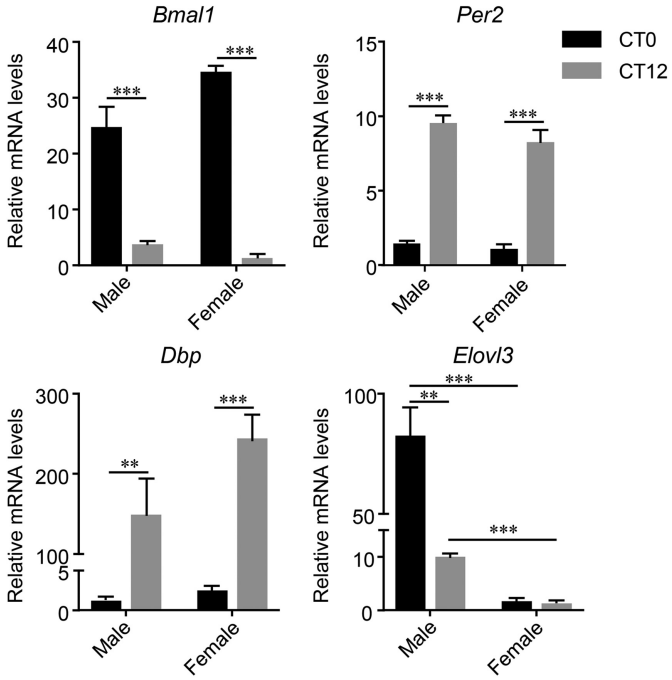

Figure 3. mRNA expression profiles of circadian clock genes and *Elovl3* in male and female mouse livers. Total RNA was extracted from the livers of male and female mice collected at CT0 and CT12, and the mRNA levels were quantified by qPCR. A two-way ANOVA Bonferroni's post-test was performed to investigate the effects of gender and time on the expression levels of the examined genes. *Asterisks* indicate significant differences. **, $p < 0.01$; ***, $p < 0.001$. *Error bars*, S.E.

observed in female mice and profound circadian changes in hepatic expression detected in male mice, along with significantly higher levels of expression (Fig. 3).

Castration reduces the circadian variations in Elovl3 in male mouse livers

To test whether androgen signaling participates in maintaining the sexually dimorphic pattern of *Elovl3* expression, we measured the mRNA expression of *Elovl3* and the other three canonical circadian clock genes (*Bmal1*, *Per2*, and *Dbp*) in castrated (*Cast*) or control (*Cont*) mouse livers at CT0 and CT12 (Fig. 4). As shown in Fig. 4*A*, control mice maintained circadian changes in serum testosterone, with high levels at CT0 and low levels at CT12. Castration significantly decreased serum testosterone concentration compared with that of the control group and resulted in a loss of rhythmicity (Fig. 4*A*). Castration clearly did not alter *Per2* and *Dbp* transcription, with respect to either circadian variation or expression level (Fig. 4*B*). Additionally, the circadian changes in *Bmal1* transcription were unaffected, despite the observed significant decrease in *Bma1l* expression levels at CT0 due to castration (Fig. 4*B*). Interestingly, castration also markedly decreased *Elovl3* mRNA expression levels at both CT0 and CT12 compared with levels observed in the control mice, although the circadian changes in *Elovl3* transcription were unchanged.

DHT injection results in Elovl3 rhythmic expression in female mouse livers

To further determine whether DHT supplementation could elicit circadian changes in *Elovl3* transcription in female mouse livers, we examined the expression of *Elovl3* and three other circadian clock genes (*Bmal1*, *Per2*, and *Dbp*) at CT0 and CT12 in female mice injected with either sesame oil (*Cont*) or DHT (Fig. 5). All three circadian clock genes (*Bmal1*, *Per2*, and *Dbp*) displayed robust circadian changes in expression in the livers obtained from either control or DHT mice (Fig. 5). DHT injection did not alter the expression levels of *Bmal1* and *Per2*, despite the observed significant decrease in *Dbp* expression at CT12 after DHT supplementation. Surprisingly, DHT injection elicited prominent circadian variations in *Elovl3* expression, with a sharp increase in *Elovl3* expression at CT0 following DHT treatment compared with that observed in the control group and a significant reduction in expression at CT12 compared with that observed at CT0 (Fig. 5).

DHT treatment increases Elovl3 expression in AML12 cells via androgen receptor signaling

To assess whether the stimulatory effect of androgen signaling on *Elovl3* expression occurred directly in mouse hepatocytes, we examined the expression levels of *Elovl3* and circadian

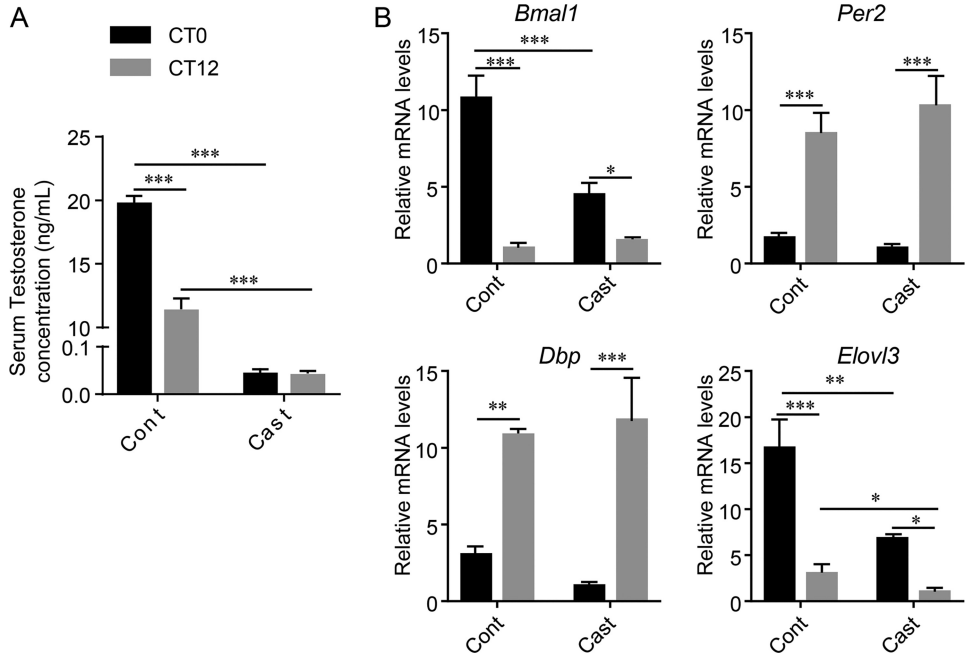

Figure 4. Effect of castration on serum testosterone concentrations and the mRNA expression profiles of circadian clock genes and *Elovl3* in male mouse livers. Serum and liver samples from control (*Cont*) and castrated (*Cast*) mice were collected at the indicated times (CT0 and CT12). *A*, serum testosterone concentrations were measured using an ELISA kit. *B*, total RNA was extracted from the livers of castrated and control mice, and the mRNA levels were quantified by qPCR. A two-way ANOVA with Bonferroni's post-test was performed to investigate the effects of castration and time on the expression of the indicated genes. *Asterisks* indicate significant differences. *, $p < 0.01$; **, $p < 0.01$; ***, $p < 0.001$. *Error bars*, S.E.

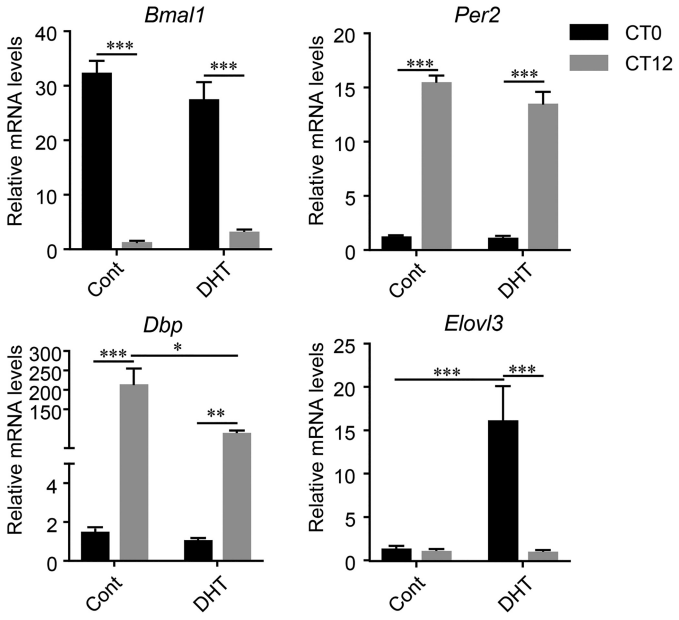

Figure 5. Effect of DHT injection on the mRNA expression profiles of circadian clock genes and *Elovl3* in female mouse livers. Total RNA was extracted from the livers of DHT-injected and control (*Cont*) female mice collected at CT0 and CT12, and the mRNA levels were quantified by qPCR. A two-way ANOVA with a Bonferroni's post-test was performed to investigate the effects of castration and time on the expression of the indicated genes. *Asterisks* indicate significant differences. *, $p < 0.01$; **, $p < 0.01$; ***, $p < 0.001$. *Error bars*, S.E.

clock genes in AML12 cells after treatment with 1 μM DHT. As shown in Fig. 6*A*, the mRNA expression of circadian clock genes (*Bmal1*, *Per2*, *Dbp*, and *Nr1d1*) did not significantly change following DHT treatment. Only minor reductions in *Dbp* and *Nr1d1* mRNA expression were observed at 2 h compared with levels at 0 h (control). DHT treatment, however, gradually increased *Elovl3* mRNA expression levels in a time-dependent manner (Fig. 6*B*). Additionally, flutamide, a selective antagonist of the androgen receptor, efficiently blocked the induction effect of DHT on *Elovl3* expression (Fig. 6*C*), providing evidence that DHT stimulates hepatic *Elovl3* expression through androgen receptor signaling.

Discussion

Several prior reports have shown that *Elovl3* transcripts exhibit a robust circadian rhythmic expression in male mouse livers (3, 4, 10). Additionally, also it was reported that mutation of the *Clock* gene completely abolished the daily rhythmicity of *Elovl3* expression (4, 10). The existing evidence suggests that the circadian clock system in the mouse liver is at least somehow linked with the rhythmic expression of *Elovl3*. Here, we further dissected the role of the circadian clock in regulating *Elovl3* cyclic transcription using *Bmal1*$^{-/-}$ mice. It is widely accepted that BMAL1 is a core transcriptional activator controlling the positive limb of circadian oscillators. In the livers of *Bmal1*$^{-/-}$ mice, *Dbp* mRNA levels are low and lose the rhythmicity normally seen under CT conditions (23). Mice with a liver-specific disruption of *Bmal1* also exhibit a nearly complete loss of liver expression of *Nr1d1* and *Dbp* (24). Additionally, two recent reports indicated that both *Bmal1* global and liver-specific knockout mice accumulated more neural lipids in the liver compared with that observed in their control group, demonstrating the significance of the circadian clock gene *Bmal1* in regulating liver lipid homeostasis (22, 25). In agreement with these previous findings, we confirmed the elevated amount of triglyceride and severely reduced *Nr1d1* and *Dbp* expression levels in the livers of *Bmal1*$^{-/-}$ mice (Fig. 1, *A–D*).

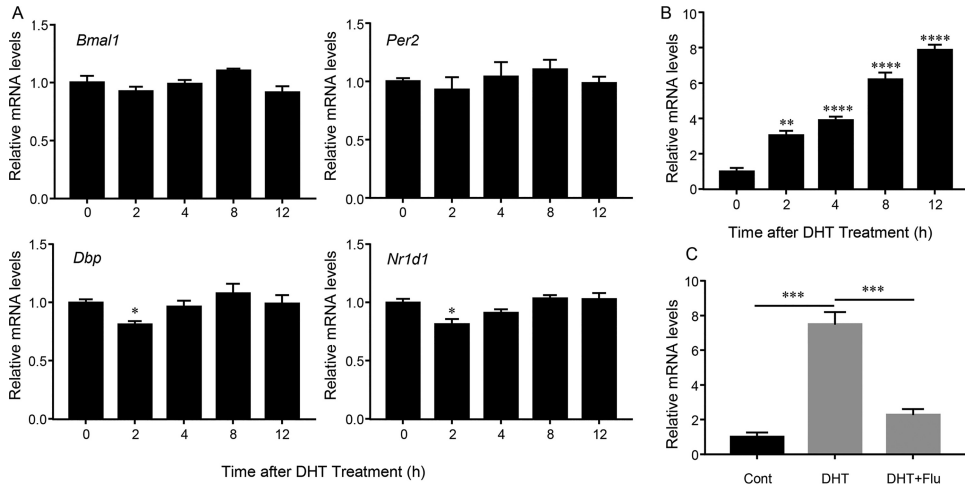

Figure 6. Blocking of the DHT stimulatory effect on *Elovl3* mRNA expression by flutamide in AML12 cells. *A* and *B*, circadian clock genes and *Elovl3* mRNA expression patterns following DHT treatment. AML12 cells were treated with 1 μM DHT, and cell samples were collected at the indicated times (0, 2, 4, 8, and 12 h). qPCR analysis was used to determine the mRNA expression levels of circadian clock genes and *Elovl3*. Each value represents the mean ± S.E. (*error bars*) of three independent determinations. A one-way ANOVA with Bonferroni's post-test was used assess the effects of DHT. *Asterisks* indicate significant differences. *, $p < 0.05$; **, $p < 0.01$; ****, $p < 0.0001$ *versus* 0 h (*Cont*). *C*, qPCR analysis of the effect of flutamide (*Flu*) on *Elovl3* expression in DHT-treated AML12 cells. AML12 cells were incubated in the presence of DHT (1 μM) with or without co-administration of Flu (100 nM), and cell samples were collected at 12 h following treatment. qPCR analysis was used to determine the mRNA expression levels of *Elovl3*. Each value represents the mean ± S.E. of three independent determinations. *Asterisks* indicate significant differences. ***, $p < 0.001$.

Importantly, our results revealed that *Elovl3* expression completely lost its circadian rhythmicity and was expressed at relatively high levels in the livers of *Bmal1*$^{-/-}$ mice (Fig. 1, *C* and *D*), in agreement with the previous findings in *Clock* mutant mice (4, 10). Interestingly, a prior study mentioned that *Elovl3*$^{-/-}$ mice gained less triglyceride in their livers after feeding with a regular or high-fat diet (7), which is consistent with our finding of an increased amount of triglyceride and *Elovl3* expression in *Bmal1*$^{-/-}$ mouse livers. Our current findings using *Bmal1*$^{-/-}$ mice have therefore provided further evidence that the cycling of *Elovl3* expression is at least in part under the control of the circadian clock, suggesting that the circadian clock may coordinate hepatic lipid metabolism through orchestrating *Elovl3* expression.

It is established that the transcriptional activity of the CLOCK-BMAL1 heterodimer reaches its maximal level during the second half of the light phase (26). Our current study, however, showed that *Elovl3* mRNA expression did not coincide with the diurnal changes in CLOCK-BMAL1 activity, and this was in agreement with other previous studies (3, 4, 10). Instead, *Elovl3* mRNA expression displayed a circadian rhythmic pattern, which was in anti-phase to two CLOCK-BMAL1–dependent genes, specifically *Nr1d1* and *Dbp* (Fig. 1, *C* and *D*). Therefore, it is reasonable to speculate that *Elovl3* rhythmic expression may be indirectly under the control of CLOCK-BMAL1 activity. Identifying the intermediates that transmit CLOCK-BMAL1–dependent information to the pathway controlling *Elovl3* gene expression is necessary. NR1D1, a component of the additional loop of the circadian clock, usually functions as a transcriptional repressor (20, 21). It has been demonstrated that NR1D1 represses *Bmal1* transcription (27). Additionally, *Nr1d1* is a CCG under the direct regulation of the CLOCK-BMAL1 heterodimer through its E-box elements (28). Intriguingly, a prior report has shown that overexpression of REV-ERBα significantly reduces *Elovl3* promoter–driven luciferase activity (4). Considering the presence of a putative RORE within the *Elovl3* promoter (Fig. 2*A*) and the anti-phase expression profile of *Elovl3* with respect to NR1D1 peak activity, it is reasonable to deduce that NR1D1 may transmit CLOCK-BMAL1 information to orchestrate the rhythmic expression of *Elovl3* in WT mouse livers through binding to the *Elovl3*-RORE. Consistent with this, our data indicated that the non-rhythmic and low expression of *Nr1d1* in *Bmal1*$^{-/-}$ mouse liver, under both ZT and CT conditions, is accompanied by consistent and relatively high levels of *Elovl3* (Fig. 1, *C* and *D*), providing further evidence that *Nr1d1* represses *Elovl3* expression. Indeed, our ChIP assay revealed that there is a circadian change of NR1D1 binding to *Elovl3*-RORE in WT mouse livers, with strong binding at CT8 and weak binding at CT20 (Fig. 2*B*), and the recruitment of NR1D1 to *Elovl3*-RORE is attenuated in *Bmal1*$^{-/-}$ mouse livers (Fig. 2*B*). Therefore, our current data provide strong evidence that NR1D1, acting as a repressor, regulates hepatic *Elovl3* rhythmic expression through binding to *Elovl3*-RORE, and diminished recruitment of NR1D1 results in elevated expression of *Elovl3* in *Bmal1*$^{-/-}$ mouse livers.

Regarding the identity of additional intermediates, SREBP1 has been proposed to be responsible for the activation of *Elovl3* in mouse liver (4). SREBP1 acts as a transcriptional integrator of circadian and nutritional cues within the liver. Prior reports indicated that SREBP1-mediated transcription is altered in *Bmal1*$^{-/-}$ and *Nr1d1*$^{-/-}$ mice (29, 30). Conversely, the daytime, food-induced resetting of the clock in WT mice has been shown to result in a 12-h phase shift in SREBP1 activation and a rescue of its rhythmic activity in *Cry1*$^{-/-}$/*Cry2*$^{-/-}$ mice (31, 32). Previous findings have shown that the overexpression of SREBP1a and -1c, but not SREBP2, robustly enhanced *Elovl3* promoter–driven luciferase activity in AML12 cells (4). Therefore, SREBP1 may act as an activator capable of stimulating *Elovl3* expression in mouse liver under the dual regulation of the circadian clock and nutritional cues. PPARα is an important

transcription factor for many target genes related to fatty acid oxidation and *de novo* lipogenesis. PPARα has previously been identified as a direct target gene of the CLOCK-BMAL1 heterodimer via an E-box–dependent mechanism (33). PPARα has also been demonstrated to act as a potent inducer of *Elovl3* expression in rodent brown adipocytes (34). Therefore, PPARα may act as a bridge connecting the circadian clock and *Elovl3* transcription in mouse liver. A prior report, however, demonstrated that there were no significant differences in *Elovl3* mRNA expression in the livers of WT and PPARα$^{-/-}$ mice at different times during the day, negating the possibility that it acts as a mediator between the circadian clock and *Elovl3* transcription in mouse liver (3).

Sexually dimorphic gene expression is a common phenomenon found between male and female livers. One elegant report showed that circadian clock system is necessary to sustain sex dimorphism in mouse liver metabolism (45). Specifically, the hepatic *Elovl3* mRNA expression becomes constitutively low, and daily variations are completely abolished in double mutant *Cry1*$^{-/-}$ *Cry2*$^{-/-}$ (*Cry*$^{-/-}$) male mice compared with WT. In addition, the hepatic *Elovl3* expression in *Cry*$^{-/-}$ males exhibits a feminized pattern of *Elovl3* expression which is similar to WT females and *Cry*$^{-/-}$ females. Using a Northern blotting approach, two prior studies have shown that *Elovl3* belongs to the sexually dimorphic gene family in mouse liver, with rhythmic expression occurring in male mouse livers and undetectable expression being observed in female mouse livers (3, 4). Consistently, our qPCR data indicated that the *Elovl3* expression levels were high and cyclical in male mouse livers, whereas expression levels were low and maintained at a constant level in female mouse livers (Fig. 3). The only discrepancy between our study and the two prior studies is that we detected low levels of *Elovl3* expression, whereas the other studies did not detect *Elovl3* transcripts in female mouse livers. We hypothesized that this inconsistency may also arise from the sensitivity of the two different methods. Specifically, qPCR is more sensitive than Northern blotting and can detect low levels of *Elovl3* expression in female mouse livers. In support of this, one other previous report identified significant levels of *Elovl3* transcripts in female mouse livers using qPCR analysis (3). Interestingly, our results indicated that almost identical expression levels of circadian clock genes (*Bmal1*, *Per2*, and *Dbp*) exist at CT0 and CT12 between male and female mouse livers (Fig. 3), suggesting that signaling pathways other than the circadian clock are involved in determining *Elovl3* expression in mouse liver. Distinct sex hormone signaling in male and female mouse livers is thought to be a major factor that drives hepatic sexual dimorphism (17). Interestingly, a prior report showed that castration resulted in undetectable expression of *Elovl3* in adult male mouse liver at ZT2, whereas control mice retained their normally high levels of *Elovl3* expression (3). Consistent with this, our data also demonstrated a large decrease in *Elovl3* mRNA expression in castrated mice at CT0 and CT12 based on a qPCR analysis (Fig. 4). In contrast, with the exception of *Bmal1*, castration did not cause a visible difference in the expression of circadian clock genes in mouse liver, ruling out the possibility that alterations in the circadian clock in castrated mice result in a reduction in *Elovl3* mRNA expression. It should be noted that castration greatly reduces serum testosterone levels in male mice (Fig. 4), raising the possibility that a lack of androgenic signaling may underlie the low expression levels of *Elovl3* in female mouse liver. Surprisingly, we found that repeated injection of DHT at either ZT12 or CT12 greatly increased *Elovl3* expression levels at CT0 in female mouse liver, inducing its circadian variation (Fig. 5). DHT injection did not significantly affect the expression of circadian clock genes, with the exception of a small decrease in *Dbp* expression levels at CT12 (Fig. 5). The above results indicate that androgen signaling may act as a driving force to elicit the sexual dimorphism of *Elovl3* expression in mouse liver. To investigate whether this DHT-driven induction of *Elovl3* mRNA in female mouse liver was a primary or secondary effect of DHT, we used qPCR to analyze the *Elovl3* mRNA levels in AML12 cells following treatment with DHT. We found that treatment of cells with 1 μM DHT significantly increased *Elovl3* expression levels in a time-dependent manner while not altering the expression of circadian clock genes (Fig. 6, *A* and *B*). We further determined whether DHT treatment activates *Elovl3* expression through androgen receptor signaling by treating cells with flutamide. Flutamide is a classical androgen antagonist that blocks androgen signaling by competitively binding to the androgen receptor (35, 36). Indeed, our qPCR results revealed that flutamide profoundly attenuated the DHT induction effect on *Elovl3* expression in AML12 cells (Fig. 6*C*), providing novel evidence that androgens activate hepatic *Elovl3* expression through androgen receptor signaling.

In conclusion, our current data suggest that the rhythmic expression of *Elovl3* is at least in part under the control of the circadian clock system through cyclic recruitment of NR1D1 to the *Elovl3* promoter. Additionally, we confirmed that the hepatic expression of *Elovl3* is sexually dimorphic, with a high and rhythmic expression occurring in male mice and a low and constant expression observed in female mice. Finally, we extended the current understanding of androgen regulation of *Elovl3* expression in mouse liver by providing evidence that androgen supplementation may restore rhythmic *Elovl3* expression in female mouse liver through androgen receptor signaling. Therefore, we propose that coordination between the circadian clock and androgen signaling is required to sustain rhythmic *Elovl3* expression in mouse liver. Although the underlying mechanism requires further investigation, our study may provide an opportunity to gain new insights into the importance of the circadian clock and androgen signaling in determining the sexual dimorphism and rhythmic expression of hepatic genes, and our results also provide novel insights into hepatic lipid homeostasis.

Experimental procedures

Animal experiments and behavior analysis

Male and female C57BL/6J mice aged 8–10 weeks were purchased from the Laboratory Animal Center of the Fourth Military Medical University (Xi'an, China). *Bmal1*$^{+/-}$ mice of the original mixed background (C57BL/6J and 129SV) were obtained from the National Resource Center of Model Mice (Nanjing, China) (23). *Bmal1*$^{+/-}$ mice were back-crossed with

C57BL/6J mice for at least five generations. For the reproductive disorders in *Bmal1*$^{-/-}$ mice, *Bmal1*$^{-/-}$ mice were generated through breeding of *Bmal1*$^{+/-}$ mice. Tail biopsies were collected for genotyping using multiplex PCR with specific primers (Common-F, 5′-GCCCACAGTCAGATTGAAAAG-3′; WT-R, 5′-CCCACATCAGCTCATTAACAA-3′; and Mut-R, 5′-GCCTGAAGAACGAGATCAGC-3′). WT littermates generated through the breeding of *Bmal1*$^{+/-}$ mice were used as a control group for the *Bmal1*$^{-/-}$ mice. Mice were housed individually in light-tight, ventilated closets in a temperature- and humidity-controlled facility with *ad libitum* access to food and water, unless otherwise stated. All mice were maintained under a 12-h/12-h LD cycle (ZT0, 0800 lights on; ZT12, 2000 lights off) for at least 2 weeks to synchronize the circadian clocks of the mice to the ambient LD cycle before the indicated experiments were performed. All animal procedures were approved and performed under the control of the Guidelines for Animal Experiments by the Committee for Ethics on Animal Care and Experiments of Northwest A&F University.

For the behavior analysis experiment, a subset of male *Bmal1*$^{-/-}$ mice and their male WT littermates ($n = 5$ for each genotype) were placed individually into an isolated LD box equipped with a passive IR sensor for 2 weeks. Following this, the mice were then released into DD under free-running conditions. CT indicates the phase of the animal's endogenous circadian rhythm while under free-running conditions, whereas CT0 marks the beginning of the subjective day, and CT12 marks the beginning of the subjective night. Locomotor activity was recorded every 5 min with the IR sensor and analyzed using ClockLab software (Actimetrics, Wilmette, IL).

For experiments involving WT and *Bmal1*$^{-/-}$ mice under ZT or CT conditions, male WT and *Bmal1*$^{-/-}$ mice aged 8–10 weeks were housed individually in light-tight, ventilated closets under a 12-h/12-h LD cycle for at least 2 weeks with *ad libitum* access to food and water. For the ZT condition experiment, male WT and *Bmal1*$^{-/-}$ mice were euthanized at six time points (ZT0, ZT4, ZT8, ZT12, ZT16, and ZT20; $n = 3$ per group for each time point). Liver samples were then collected for total RNA extraction. For the CT condition experiment, male WT and *Bmal1*$^{-/-}$ mice were housed as described above and then released into DD under free-running conditions. At the start of the second day under CT conditions, male WT and *Bmal1*$^{-/-}$ mice were euthanized at six time points (CT0, CT4, CT8, CT12, CT16, CT20; $n = 3$ per group for each time point). Liver samples were then collected for total RNA extraction.

For the male and female mouse experiment, male and female WT mice aged 8–10 weeks were housed individually in light-tight, ventilated closets under a 12-h/12-h LD cycle for at least 2 weeks with *ad libitum* access to food and water. The mice were then released into DD under free-running conditions. Beginning on the second day under CT conditions, male and female WT mice were euthanized at two time points (CT0 and CT12; $n = 3$ per group for each time point). Liver samples were then collected for total RNA extraction.

For the castration experiment, male WT mice aged 8–10 weeks were castrated or sham-operated (control) ($n = 6$ mice/group). All operative procedures were performed under pentobarbital anesthesia (50 mg/kg body weight, by intraperitoneal injection). An incision was first made in the wall of the abdomen. The testis with the epididymis was then removed following seminal duct ligation. After this operation, the mice were housed individually in light-tight, ventilated closets under a 12-h/12-h LD cycle for 2 weeks. The mice were then released into DD under free-running conditions. At the start of the second day under CT conditions, the mice from the castrated and control groups were euthanized at two time points (CT0 and CT12; $n = 3$ per group for each time point). Blood samples were then collected for serum testosterone level measurement using an ELISA kit, and liver samples were collected for total RNA extraction.

For the DHT (HY-A0120, MedChemExpress, Monmouth Junction, NJ) treatment experiment, female WT mice aged 8–10 weeks were randomly divided into two groups (DHT and control; $n = 6$ mice/group). First, 9 mg of DHT was dissolved into 30 ml of sesame oil to prepare a DHT solution (300 μg/ml). The mice in the two groups were housed individually in light-tight, ventilated closets under a 12-h/12-h LD cycle for 2 weeks. At the start of the second week during the LD cycle, mice in the DHT treatment group were injected subcutaneously with DHT (2 mg/kg body weight) every day at ZT12 (a total of seven injections), whereas the control mice were injected with a corresponding volume of sesame oil based on their body weights (37). After 2 weeks under the LD cycle, the mice were released into DD under free-running conditions. The DHT and control mice received one further injection of DHT or sesame oil, respectively, at CT12 on the first day under DD conditions. At the start of the second day under CT conditions, mice in the DHT and control groups were euthanized at two time points (CT0 and CT12; $n = 3$ per group). Liver samples were then collected for total RNA extraction.

Immunohistochemistry

Immunohistochemistry procedures were performed as described previously (38). Liver specimens from male WT and *Bmal1*$^{-/-}$ mice were collected at ZT0 and ZT12 and fixed with 4% paraformaldehyde and then embedded in paraffin-wax using standard protocols. Five-micrometer-thick sections were deparaffinized with xylene and ethanol, and then antigen-retrieval was performed by pressure cooking in a citric acid salt mixture (1.8 mM citrate and 8.2 mM sodium citrate, pH 6.0) for 15 min. Sections were then immersed in PBS containing 0.2% Triton X-100. Prior to diaminobenzidine (DAB) labeling, immunohistochemical staining of the slices was performed using an UltraSensitive^{TM} SP (rabbit) IHC kit (Fuzhou Maixin Biotech, Fuzhou, China). Briefly, the sections were pretreated with 3% hydrogen peroxide solution (Reagent A in the IHC kit) for 15 min and then blocked with 10% goat serum (Reagent B in the IHC kit) for 1 h at 37 °C. The primary antibody to BMAL1 (Abcam, ab93806, Cambridge, UK) was diluted in PBS (1:1000 dilution) containing 1% BSA, 1% fetal bovine serum, and 0.1% Triton X-100. Following overnight incubation at 4 °C, the sections were washed extensively with PBS containing 0.3% Tween 20. The samples were then incubated with a goat anti-rabbit secondary antibody conjugated to biotin (reagent C in the IHC kit), diluted in the same PBS solution as the primary antibody, and then incubated for 1 h at 37 °C and washed again. For DAB labeling, the sections were incubated with horseradish

Table 1
Primer sequences for ChIP assays

Gene	Forward primer (5′–3′)	Reverse primer (5′–3′)	Product size
			bp
mBmal1 RORE	AGCGGATTGGTCGGAAAGT	ACCTCCGTCCCTGACCTACT	72
mElovl3 RORE	TACGTTCAGACTGGGAAGGG	AAAAATGGGGTCACCCTCTGG	124
mElovl3 intron1	GGATTAGCGTGTCCCACACA	CGTCTGGGACGATTTAGGGC	136

Table 2
Primer sequences for the targeted genes in qPCR

Gene	Accession number	Forward (5′–3′)	Product size
			bp
mBmal1	NM_007489.4	F: AGGCGTCGGGACAAAATGAACA R: TGGGTTGGTGGCACCTCTCA	147
mNr1d1	NM_145434.4	F: TGGCATGGTGCTACTGTGTAAGG R: ATATTCTGTTGGATGCTCCGGCG	114
mPer2	NM_011066.3	F: GAAAGCTGTCACCACCATAGAA R: AACTCGCACTTCCTTTTCAGG	186
mDbp	NM_016974.3	F: AATGACCTTTGAACCTGATCCCGCT R: GCTCCAGTACTTCTCATCCTTCTGT	175
mElovl3	NM_007703.2	F: GGACCTGATGCAACCCTATG R: CCAACAACGATGAGCAACAG	117
mTbp	NM_013684.3	F: TGTATCTACCGTGAATCTTGGC R: CAGTTGTCCGTGGCTCTCTT	128
m36b4	NM_007475.5	F: CTCACTGAGATTCGGGATATG R: CTCCCACCTTGTCTCCAGTC	223

peroxidase–streptavidin (Reagent D in the IHC kit) for 30 min at 37 °C, followed by two sequential washes with PBS in 0.3% Tween 20 and 50 mM Tris-HCl (pH 7.4) for 5 min at room temperature. DAB development was performed by incubation with a 0.02% DAB (D5637, Sigma-Aldrich) solution in 50 mM Tris-HCl, 0.001% H_2O_2 (pH 7.4) at room temperature for 2 min. Normal rabbit IgG (SC-2763, 1:100 dilution, Santa Cruz Biotechnology, Inc., Dallas, TX) was used to replace the BMAL1 antibody as a negative control.

Protein extraction and Western blotting

The preparation of lysates from liver tissues and Western blotting procedures was performed as described previously (39). Protein extracts were prepared from equal amounts of liver tissue collected from male WT and *Bmal1*$^{-/-}$ mice at ZT0 and ZT12 and lysed in Laemmli SDS buffer supplemented with protease inhibitors (Roche, Basel, Switzerland). The protein concentration was determined using a bicinchoninic acid assay protein detection kit (KeyGen Biotech, Nanjing, China). Equal amounts of total protein (25 μg) from each sample were separated by 12% SDS-PAGE and electrically transferred to polyvinylidene difluoride membranes (EMD Millipore, Billerica, MA). The membranes were blocked in a 10% nonfat milk powder solution for 1 h in TBS containing 0.5% Tween 20 at room temperature, after which the membranes were incubated overnight at 4 °C with the anti-BMAL1 antibody (1:2000 dilution; Abcam) or an anti-β-actin antibody (1:2000 dilution; Sungene Biotech, Tianjin, China) diluted in TBST. On the second day, the membranes were washed and then incubated with horseradish peroxidase–conjugated secondary antibody (1:4000 dilution; Zhong Shan Jinqiao Biological Technology Co., Beijing, China) diluted in TBST for 1 h at room temperature. The peroxidase activity was detected using a WesternBright ECL horseradish peroxidase substrate kit (Advansta, Menlo Park, CA). Finally, the immunoreactive bands were visualized using a gel imaging analyzer (Tanon Biotech, Shanghai, China).

Oil Red O staining and hepatic triglyceride assay

Male WT and *Bmal1*$^{-/-}$ mice aged 8–10 weeks were housed individually in light-tight, ventilated closets under one 12-h/12-h LD cycle for at least 2 weeks with *ad libitum* access to food and water. The liver samples of mice were collected at ZT10 ($n = 8$ for each genotype). Oil Red O staining was performed according to a previous report with minor modifications (22). Briefly, frozen sections (8 μM) were prepared from snap-frozen liver tissues and fixed in 10% buffered formalin for 10 min. The sections were then stained with freshly prepared 0.5% Oil Red O in isopropyl alcohol at 37 °C for 25 min. After rinsing with 60% isopropyl alcohol, the sections were further counterstained with hematoxylin for 5 s. Hepatic lipids were extracted according to the methods of Folch *et al.* (40). The extract was dissolved in isopropyl alcohol and subsequently quantified using Wako kits (Wako Pure Chemical Industries, Ltd.).

ChIP assay

ChIP assay was performed using a SimpleChIP® enzymatic chromatin IP kit (Cell Signaling, catalog no. 9003) according to the manufacturer's protocol. Briefly, livers from WT and *Bmal1*$^{-/-}$ mice were harvested immediately at CT8 and CT20 after euthanasia ($n = 4$ for each time point of genotype). The shredded mouse liver was resuspended in cold PBS containing 1 mM proteinase, followed by treatment with 1% formaldehyde (for chromatin cross-linking) for 20 min at room temperature. Chromatin with a length of ~150–900 bp was obtained after digestion with micrococcal nuclease and shearing with ultrasonication. For each reaction, 10 μg of fragmented chromatin was immunoprecipitated with rabbit anti-NR1D1 (Cell Signaling, catalog no. 13418) or normal rabbit IgG (control, Cell Signaling, catalog no. 2729) by overnight incubation at 4 °C. Protein G magnetic beads were then added to each ChIP sample, and samples were then incubated for 2 h at 4 °C with shaking to allow precipitation of the immunocomplexes. After elution, decross-linking, and purification, the purified DNAs were used as a template for qPCR with specific primers (Table 1).

RNA extraction and quantitative real-time PCR

Liver tissues or AML12 cell samples were harvested at the indicated time points. Total RNA was extracted using TRIzol reagent (TaKaRa, Dalian, China), and the RNA samples were treated with RNase-free DNase (TianGen, Beijing, China). The cDNAs were generated using a PrimeScript RT Reagent Kit (TaKaRa). The primer sets used for qPCR are listed in Table 2. All primer sets were designed to span introns to avoid amplifying products from genomic DNA. qPCR was performed on the

CFX96 RT-qPCR system (Bio-Rad) using the SYBR Premix Ex TaqII kit (TaKaRa) with a 20-μl reaction volume containing 10 ng of cDNA and a 200 nM concentration of the specific primers, as described previously (41). Melting peaks were determined using a melting curve analysis to ensure the amplification and the generation of a single product. All reactions were performed in triplicate and displayed amplification efficiencies between 80 and 120%. The $2^{-\Delta\Delta Ct}$ method was used to quantify gene expression. *Tbp* and *36b4* were used as internal reference genes, and the geometric average of these two reference genes was used to normalize the relative expression according to a previous report (42).

Cell culture and treatment

The hepatocyte cell line AML12, generated from the liver of TGFα-transgenic mice, was kindly provided by Stem Cell Bank, Chinese Academy of Sciences (43). The cells were plated (5×10^5 cells/dish) on 35-mm collagen-coated dishes (Thermo Fisher Scientific) in Dulbecco's modified Eagle's medium/Ham's F-12 (Thermo Fisher Scientific) supplemented with 10% FBS (Gibco), 1× insulin-transferrin-selenium liquid medium supplement (ITS, Sigma-Aldrich), 0.1 μM dexamethasone (Sigma-Aldrich), and 1× antibiotic-antimycotic (containing penicillin, streptomycin, and amphotericin B; Thermo Fisher Scientific) in a humidified atmosphere of 95% air and 5% CO_2 at 37 °C. Cells were cultured for 24 h to reach confluence. For the DHT treatment experiment, cells were then treated with 1 μM DHT. Cell samples were collected for total RNA extraction at 0, 2, 4, 8, and 12 h after the DHT treatment. For the flutamide-blocking experiment, AML12 cells were incubated in the presence of DHT (1 μM) with or without co-administration of flutamide (100 nM), and cell samples were collected for total RNA extraction at 12 h following treatment.

Data analysis and statistics

Data are expressed as the means ± S.E. of at least three independent experiments, each performed with triplicate samples. The circadian rhythmicity in gene expression was determined by the single Cosinor method using Time Series Single 6.3 (Expert Soft Tech, Richelieu, France). Rhythmicity was defined by a confidence region for the mesor using a *t* distribution with the level of significance taken as ≤5%. Other statistical analyses were performed using Student's *t* test, a one-way ANOVA, or a two-way ANOVA, as indicated, using SigmaPlot version 12.0 (Systat Software, San Jose, CA). Differences were considered significant at $p < 0.05$.

Author contributions—H. C. and Y. J. conceptualization; H. C. formal analysis; H. C. and Y. J. supervision; H. C. funding acquisition; H. C., L. G., and A. W. validation; H. C., L. G., and D. Y. investigation; H. C., L. G., D. Y., Y. X., M. Z., and C. L. methodology; H. C. writing-original draft; H. C. and Y. J. project administration; L. G. data curation; L. G. and Y. J. writing-review and editing.

References

1. Tvrdik, P., Asadi, A., Kozak, L. P., Nedergaard, J., Cannon, B., and Jacobsson, A. (1997) *Cig30*, a mouse member of a novel membrane protein gene family, is involved in the recruitment of brown adipose tissue. *J. Biol. Chem.* **272,** 31738–31746 CrossRef Medline
2. Ji, L., Gupta, M., and Feldman, B. J. (2016) Vitamin D regulates fatty acid composition in subcutaneous adipose tissue through Elovl3. *Endocrinology* **157,** 91–97 CrossRef Medline
3. Brolinson, A., Fourcade, S., Jakobsson, A., Pujol, A., and Jacobsson, A. (2008) Steroid hormones control circadian *Elovl3* expression in mouse liver. *Endocrinology* **149,** 3158–3166 CrossRef Medline
4. Anzulovich, A., Mir, A., Brewer, M., Ferreyra, G., Vinson, C., and Baler, R. (2006) *Elovl3*: a model gene to dissect homeostatic links between the circadian clock and nutritional status. *J. Lipid. Res.* **47,** 2690–2700 CrossRef Medline
5. Westerberg, R., Tvrdik, P., Undén, A. B., Månsson, J. E., Norlén, L., Jakobsson, A., Holleran, W. H., Elias, P. M., Asadi, A., Flodby, P., Toftgård, R., Capecchi, M. R., and Jacobsson, A. (2004) Role for ELOVL3 and fatty acid chain length in development of hair and skin function. *J. Biol. Chem.* **279,** 5621–5629 CrossRef Medline
6. Westerberg, R., Månsson, J. E., Golozoubova, V., Shabalina, I. G., Backlund, E. C., Tvrdik, P., Retterstøl, K., Capecchi, M. R., and Jacobsson, A. (2006) ELOVL3 is an important component for early onset of lipid recruitment in brown adipose tissue. *J. Biol. Chem.* **281,** 4958–4968 CrossRef Medline
7. Zadravec, D., Brolinson, A., Fisher, R. M., Carneheim, C., Csikasz, R. I., Bertrand-Michel, J., Borén, J., Guillou, H., Rudling, M., and Jacobsson, A. (2010) Ablation of the very-long-chain fatty acid elongase ELOVL3 in mice leads to constrained lipid storage and resistance to diet-induced obesity. *FASEB J.* **24,** 4366–4377 CrossRef Medline
8. Xu, J., Liu, D., Yin, H., Tong, H., Li, S., and Yan, Y. (2018) Fatty acids promote bovine skeletal muscle satellite cell differentiation by regulating ELOVL3 expression. *Cell Tissue Res.* **373,** 499–508 CrossRef Medline
9. Kobayashi, T., and Fujimori, K. (2012) Very long-chain-fatty acids enhance adipogenesis through coregulation of Elovl3 and PPARγ in 3T3-L1 cells. *Am. J. Physiol. Endocrinol. Metab.* **302,** E1461–E1471 CrossRef Medline
10. Panda, S., Antoch, M. P., Miller, B. H., Su, A. I., Schook, A. B., Straume, M., Schultz, P. G., Kay, S. A., Takahashi, J. S., and Hogenesch, J. B. (2002) Coordinated transcription of key pathways in the mouse by the circadian clock. *Cell* **109,** 307–320 CrossRef Medline
11. Dibner, C., Schibler, U., and Albrecht, U. (2010) The mammalian circadian timing system: organization and coordination of central and peripheral clocks. *Annu. Rev. Physiol.* **72,** 517–549 CrossRef Medline
12. Pilorz, V., Helfrich-Förster, C., and Oster, H. (2018) The role of the circadian clock system in physiology. *Pflugers Arch.* **470,** 227–239 CrossRef Medline
13. Ralph, M. R., Foster, R. G., Davis, F. C., and Menaker, M. (1990) Transplanted suprachiasmatic nucleus determines circadian period. *Science* **247,** 975–978 CrossRef Medline
14. Albrecht, U. (2012) Timing to perfection: the biology of central and peripheral circadian clocks. *Neuron* **74,** 246–260 CrossRef Medline
15. Henson, M. A., To, T. L., Herzog, E. D., and Doyle, F. J., 3rd (2007) A molecular model for intercellular synchronization in the mammalian circadian clock. *Biophys. J.* **92,** 3792–3803 CrossRef Medline
16. Huang, N., Chelliah, Y., Shan, Y., Taylor, C. A., Yoo, S. H., Partch, C., Green, C. B., Zhang, H., and Takahashi, J. S. (2012) Crystal structure of the heterodimeric CLOCK:BMAL1 transcriptional activator complex. *Science* **337,** 189–194 CrossRef Medline
17. van Nas, A., Guhathakurta, D., Wang, S. S., Yehya, N., Horvath, S., Zhang, B., Ingram-Drake, L., Chaudhuri, G., Schadt, E. E., Drake, T. A., Arnold, A. P., and Lusis, A. J. (2009) Elucidating the role of gonadal hormones in sexually dimorphic gene coexpression networks. *Endocrinology* **150,** 1235–1249 CrossRef Medline
18. Jansson, J. O., Edén, S., and Isaksson, O. (1985) Sexual dimorphism in the control of growth hormone secretion. *Endocr. Rev.* **6,** 128–150 CrossRef Medline
19. Zheng, D., Wang, X., Antonson, P., Gustafsson, J. Å., and Li, Z. (2018) Genomics of sex hormone receptor signaling in hepatic sexual dimorphism. *Mol. Cell. Endocrinol.* **471,** 33–41 CrossRef Medline

20. Coste, H., and Rodríguez, J. C. (2002) Orphan nuclear hormone receptor Rev-erbα regulates the human apolipoprotein CIII promoter. *J. Biol. Chem.* **277,** 27120–27129 CrossRef Medline
21. Zamir, I., Zhang, J., and Lazar, M. A. (1997) Stoichiometric and steric principles governing repression by nuclear hormone receptors. *Genes Dev.* **11,** 835–846 CrossRef Medline
22. Bugge, A., Feng, D., Everett, L. J., Briggs, E. R., Mullican, S. E., Wang, F., Jager, J., and Lazar, M. A. (2012) Rev-erbα and Rev-erbβ coordinately protect the circadian clock and normal metabolic function. *Genes Dev.* **26,** 657–667 CrossRef Medline
23. Bunger, M. K., Wilsbacher, L. D., Moran, S. M., Clendenin, C., Radcliffe, L. A., Hogenesch, J. B., Simon, M. C., Takahashi, J. S., and Bradfield, C. A. (2000) Mop3 is an essential component of the master circadian pacemaker in mammals. *Cell* **103,** 1009–1017 CrossRef Medline
24. Lamia, K. A., Storch, K. F., and Weitz, C. J. (2008) Physiological significance of a peripheral tissue circadian clock. *Proc. Natl. Acad. Sci. U. S. A.* **105,** 15172–15177 CrossRef Medline
25. Shimba, S., Ogawa, T., Hitosugi, S., Ichihashi, Y., Nakadaira, Y., Kobayashi, M., Tezuka, M., Kosuge, Y., Ishige, K., Ito, Y., Komiyama, K., Okamatsu-Ogura, Y., Kimura, K., and Saito, M. (2011) Deficient of a clock gene, brain and muscle arnt-like protein-1 (BMAL1), induces dyslipidemia and ectopic fat formation. *PLoS One* **6,** e25231 CrossRef Medline
26. Young, M. W., and Kay, S. A. (2001) Time zones: a comparative genetics of circadian clocks. *Nat. Rev. Genet.* **2,** 702–715 CrossRef Medline
27. Preitner, N., Damiola, F., Lopez Molina, L., Zakany, J., Duboule, D., Albrecht, U., and Schibler, U. (2002) The orphan nuclear receptor REV-ERBα controls circadian transcription within the positive limb of the mammalian circadian oscillator. *Cell* **110,** 251–260 CrossRef Medline
28. Triqueneaux, G., Thenot, S., Kakizawa, T., Antoch, M. P., Safi, R., Takahashi, J. S., Delaunay, F., and Laudet, V. (2004) The orphan receptor *Rev-erbα* gene is a target of the circadian clock pacemaker. *J. Mol. Endocrinol.* **33,** 585–608 CrossRef Medline
29. Gilardi, F., Migliavacca, E., Naldi, A., Baruchet, M., Canella, D., Le Martelot, G., Guex, N., Desvergne, B., and CycliX Consortium (2014) Genome-wide analysis of SREBP1 activity around the clock reveals its combined dependency on nutrient and circadian signals. *PLoS Genet.* **10,** e1004155 CrossRef Medline
30. Le Martelot, G., Claudel, T., Gatfield, D., Schaad, O., Kornmann, B., Lo Sasso, G., Moschetta, A., and Schibler, U. (2009) REV-ERBα participates in circadian SREBP signaling and bile acid homeostasis. *PLoS Biol.* **7,** e1000181 CrossRef Medline
31. Brewer, M., Lange, D., Baler, R., and Anzulovich, A. (2005) SREBP-1 as a transcriptional integrator of circadian and nutritional cues in the liver. *J. Biol. Rhythms* **20,** 195–205 CrossRef Medline
32. Vollmers, C., Gill, S., DiTacchio, L., Pulivarthy, S. R., Le, H. D., and Panda, S. (2009) Time of feeding and the intrinsic circadian clock drive rhythms in hepatic gene expression. *Proc. Natl. Acad. Sci. U.S.A.* **106,** 21453–21458 CrossRef Medline
33. Oishi, K., Shirai, H., and Ishida, N. (2005) CLOCK is involved in the circadian transactivation of peroxisome-proliferator-activated receptor α (*PPARα*) in mice. *Biochem. J.* **386,** 575–581 CrossRef Medline
34. Jakobsson, A., Jörgensen, J. A., and Jacobsson, A. (2005) Differential regulation of fatty acid elongation enzymes in brown adipocytes implies a unique role for *Elovl3* during increased fatty acid oxidation. *Am. J. Physiol. Endocrinol. Metab.* **289,** E517–E526 CrossRef Medline
35. Labrie, F. (1993) Mechanism of action and pure antiandrogenic properties of flutamide. *Cancer* **72,** 3816–3827 CrossRef Medline
36. Ilagan, R., Zhang, L. J., Pottratz, J., Le, K., Salas, S., Iyer, M., Wu, L., Gambhir, S. S., and Carey, M. (2005) Imaging androgen receptor function during flutamide treatment in the LAPC9 xenograft model. *Mol. Cancer Ther.* **4,** 1662–1669 CrossRef Medline
37. De Giorgio, M. R., Yoshioka, M., and St-Amand, J. (2010) A single dose of dihydrotestosterone induced a myogenic transcriptional program in female intra-abdominal adipose tissue. *J. Steroid Biochem. Mol. Biol.* **122,** 53–64 CrossRef Medline
38. Chao, H. W., Doi, M., Fustin, J. M., Chen, H., Murase, K., Maeda, Y., Hayashi, H., Tanaka, R., Sugawa, M., Mizukuchi, N., Yamaguchi, Y., Yasunaga, J. I., Matsuoka, M., Sakai, M., Matsumoto, M., *et al.* (2017) Circadian clock regulates hepatic polyploidy by modulating Mkp1-Erk1/2 signaling pathway. *Nat. Commun.* **8,** 2238 CrossRef Medline
39. Xiong, Y., Chen, H., Lin, P., Wang, A., Wang, L., and Jin, Y. (2017) ATF6 knockdown decreases apoptosis, arrests the S phase of the cell cycle, and increases steroid hormone production in mouse granulosa cells. *Am. J. Physiol. Cell Physiol.* **312,** C341–C353 CrossRef Medline
40. Folch, J., Lees, M., and Sloane Stanley, G. H. (1957) A simple method for the isolation and purification of total lipides from animal tissues. *J. Biol. Chem.* **226,** 497–509 Medline
41. Yang, D., Jiang, T., Liu, J., Zhang, B., Lin, P., Chen, H., Zhou, D., Tang, K., Wang, A., and Jin, Y. (2018) CREB3 regulatory factor-mTOR-autophagy regulates goat endometrial function during early pregnancy. *Biol. Reprod.* **98,** 713–721 CrossRef Medline
42. Vandesompele, J., De Preter, K., Pattyn, F., Poppe, B., Van Roy, N., De Paepe, A., and Speleman, F. (2002) Accurate normalization of real-time quantitative RT-PCR data by geometric averaging of multiple internal control genes. *Genome Biol.* **3,** RESEARCH0034 Medline
43. Wu, J. C., Merlino, G., and Fausto, N. (1994) Establishment and characterization of differentiated, nontransformed hepatocyte cell-lines derived from mice transgenic for transforming growth factor α. *Proc. Natl. Acad. Sci. U.S.A.* **91,** 674–678 CrossRef Medline
44. Khan, A., Fornes, O., Stigliani, A., Gheorghe, M., Castro-Mondragon, J. A., van der Lee, R., Bessy, A., Chèneby, J., Kulkarni, S. R., Tan, G., Baranasic, D., Arenillas, D. J., Sandelin, A., Vandepoele, K., Lenhard, B., Ballester, B., Wasserman, W. W., Parcy, F., and Mathelier, A. (2018) JASPAR 2018: update of the open-access database of transcription factor binding profiles and its web framework. *Nucleic Acids Res.* **46,** D260–D266 CrossRef Medline
45. Bur, I. M., Cohen-Solal, A. M., Carmignac, D., Abecassis, P. Y., Chauvet, N., Martin, A. O., van der Horst, G. T. J., Robinson, I. C. A. F., Maurel, P., Mollard, P., and Bonnefont, X. (2009) The circadian clock components CRY1 and CRY2 are necessary to sustain sex dimorphism in mouse liver metabolism. *J. Biol. Chem.* **284,** 9066–9073 CrossRef Medline